Solid Earth, 14, 515–528, 2023
https://doi.org/10.5194/se-14-515-2023

Solid Earth Open Access EGU

Geometry and topology of a Polish Outer Carpathian digital-elevation-model-interpreted lineament network in the context of regional tectonics

Maciej Kania and Mateusz Szczęch

Institute of Geological Sciences, Faculty of Geography and Geology, Jagiellonian University in Kraków, Kraków, Poland

Correspondence: Maciej Kania (maciej.kania@uj.edu.pl)

Received: 25 November 2022 – Discussion started: 12 December 2022
Revised: 6 March 2023 – Accepted: 5 April 2023 – Published: 12 May 2023

Abstract. The Polish part of the Western Outer Carpathian lineament network was analysed based on the Global Multi-resolution Terrain Elevation Data 2010 (GMTED2010) digital elevation model. Lineaments were identified in the visual screening of the hillshade model. To the best of our knowledge, no one has studied the geometrical properties of the network in relation to the topological ones. The NetworkGT QGIS toolbox was applied to identify the nodes and branches of the network as well as to calculate the topology parameters. Our aim was to find differences between the western and eastern parts of the Western Outer Carpathians; therefore, the analyses were carried out in six sectors chosen based on the geographical subdivision in the geological context: three in the north, mainly the Silesian unit, and three in the south, mainly the Magura unit. We found general agreement of the identified network with the photo-lineament map; however, some of the photo-lineaments are not confirmed by a digital elevation model (DEM). We found that the topological parameters of the networks change from west to east but not from north to south. There are areas of increased interconnectivity, especially the Nowy Sącz Basin, where the lineament network may reflect a complicated system of cross-cutting, deep-rooted fault zones in the basement.

1 Introduction

Remote-sensing imagery is an important source of data in regional tectonics, and its importance has been growing in recent years. Since the 1970s, there have been multispectral satellite photos of the Earth's surface applied mainly in mineral mapping (e.g. van der Meer et al., 2012) as well as in tectonic studies (e.g. Leech et al., 2003). The Shuttle Radar Topography Mission (SRTM) resulted in the first remote-sensing digital elevation model of most of the continental surface of the planet, with immense potential for application in geology (Yang et al., 2011). Then, new superior-resolution and superior-quality models were created on both the global (satellite) and local scale (mainly airborne lidar scanning). Digital elevation models are especially useful in areas with lush vegetation. The application of lidar in the Carpathians' flysch-type mountains in geological interpretations was shown, for example, in Kania and Szczęch (2022).

Our previous study (Kania and Szczęch, 2020), based on the interpretation of the model augmented with field geological mapping (Szczęch and Cieszkowski, 2021), showed how a lineament network can be interpreted in topological and geometrical terms. This paper presents DEM-based geometrical and topological analyses of a regional scale lineament network to find how this is reflected in the tectonic structure of the Western Carpathians. Previous studies of the Carpathian lineaments were mainly focused on lineament strike distribution (e.g. Doktór and Graniczny, 1982, 1983; Doktór et al., 1985, 1990, 2002; Bażyński et al., 1986; Graniczny and Mizerski, 2003); therefore, we decided to add an interconnectivity aspect in terms of the topological parameters (Valentini et al., 2007; Sanderson and Nixon, 2015; Thiele et al., 2016) as a way of better understanding the structural problems. There were two problems which we tried to address. The first aim was to find out if and how the deep-rooted lineaments (fault zones) influence lineament network pattern on the surface. Our hypothesis was that these deep-rooted features are expressed in the network independently of

the contemporary observed Carpathian nappe stacked structure. The second question was if and how the lineament network properties change in the west–east profile. Most of the Carpathian-related studies are geographically organized in mountain arc parallel belts, reflecting the main tectonostratigraphic units, now forming nappes which were developed from sedimentary basins during the Carpathian flysch depositions. We decided to keep this subdivision, although combining this with physiographical subdivisions into sectors with borders perpendicular to the Carpathian belt.

2 Previous research on the Polish Outer Carpathian lineaments

The fact that dislocation lines perpendicular to the Carpathian arc are related to the deep basement and are significantly older than the Carpathians themselves was stated even before the remote-sensing era (Teisseyre, 1907). The first modern attempts to interpret lineaments in the Polish Carpathians were based on the Landsat MSS (Multispectral Scanner) imagery and Heat Capacity Mapping Mission satellite and reported together with data from the whole territory of Poland on a photogeological map at a 1 : 1 000 000 scale (Bażyński et al., 1986; Graniczny and Mizerski, 2003). The main lineament systems of the Western Carpathians in the context of structural geology were shown by Doktór and Graniczny (1983) and Doktór et al. (1985). The results of satellite imagery lineament detections were then correlated with geophysical data proving relationships between the surface, neotectonic processes and deep Carpathian basement structure (Motyl-Rakowska and Ślączka, 1984; Doktór et al., 1990). Airborne radar data were applied in tectonic analysis of the Carpathians, resulting in 17 000 short lineaments that were the basis of the lineament density map (Doktór et al., 2002). The interpretation of SRTM hillshading visualization was performed by Chodyń (2004) in the limited area in the Beskid Wyspowy Mts. A comparison of Landsat MSS and SRTM data by Ozimkowski (2008) showed that whilst the main faults can be related to lineaments, there are still numerous lineaments without geological explanation. In the last few years lidar high-resolution digital elevation models have become available for the Polish Carpathians allowing more regional-scale lineament network analysis and their interpretation as fault-related features (Kania and Szczęch, 2020, 2022; Szczęch and Cieszkowski, 2021; Barmuta et al., 2021; Sikora, 2022)

3 Study area

The choice of the study area was based on the physiogeographical subdivision of Poland by Solon et al. (2018). The following macro-regions were selected: the West Beskidian Foothills, the Western Beskids, the Orawa–Podhale Basin, the mid-Beskidian Foothills, and the mid-Beskids (Fig. 1). These five regions, with a total area of 17 437 km^2, cover most of the Polish part of the Outer Carpathians, excluding a small part of the Eastern Outer Carpathians located in Poland.

3.1 Geological setting of the study area

The research area is located in the Polish sector of the Western Outer Carpathians (Mahel', 1974; Książkiewicz, 1977; Ślączka et al., 2006; Fig. 2). Tectonically, it contacts the Pieniny Klippen Belt from the south, which is a border between the Outer and the Central Carpathians (Książkiewicz, 1977; Plašienka, 2018; Golonka et al., 2019, 2021). The basement under the Western Outer Carpathians is formed of two blocks: the Brunovistulicum and the Małopolska Massif. These are separated by a major tectonic zone – the Kraków–Lubliniec Fault (Fig. 2b, Żaba, 1999; Żelaźniewicz, 2011), which is cut by numerous other deep rooted lineaments (Doktór et al., 1985). The Outer Carpathians are built mainly of flysch deposits, whose thickness is approximately 6000 m, and thus they are also referred to as the Flysch Carpathians (Książkiewicz, 1977; Golonka et al., 2005, 2021; Ślączka et al., 2006). These deposits are Late Jurassic–early Miocene in age and are mainly deep-sea sediments deposited by the gravity flow in the several sedimentary basins of the northern Tethys, separated by ridges (Książkiewicz, 1977; Golonka et al., 2005, 2021; Ślączka et al., 2006). The thrust of the Central Carpathian block to the north on the European Platform blocks – the Brunovistulicum and the Małopolska Massif (Żaba, 1999) – led to the formation of the synorogenic stage accretionary prism. The sediments deposited in the basins were folded and thrusted one upon another, creating the sequence of nappes in the Miocene. Going from the south there are the Magura Nappe, the Dukla Nappe, the Fore-Magura group of nappes, the Silesian Nappe, the Sub-Silesian Nappe, and the Skole Nappe (Mahel', 1974; Książkiewicz, 1977; Golonka et al., 2005, 2019; Ślączka et al., 2006). The deposits of the Outer Carpathians are thrust over the Miocene molasses filling the Carpathian Foredeep, which was deposited on the front of the Outer Carpathian orogenic belt thrusting over the North European Platform (Ślączka et al., 2006; Oszczypko, 2006).

3.2 Analysis of the sectors

We used the morphometry subdivision of Poland (Solon et al., 2018) to define the area, based on the subprovinces of the Western Outer Carpathians in the area of Poland and a small band of northern sub-Carpathian subprovinces on the border of the Carpathians in the geological sense (Carpathian overthrust on the Foredeep sediments), according to Lexa et al. (2000). The subdivision of the outer Carpathian belt is mostly used in the geology basis on the tectonostratigraphic units (nappes). This subdivision, however, does not allow differences in lineament systems parallel to the belt to be

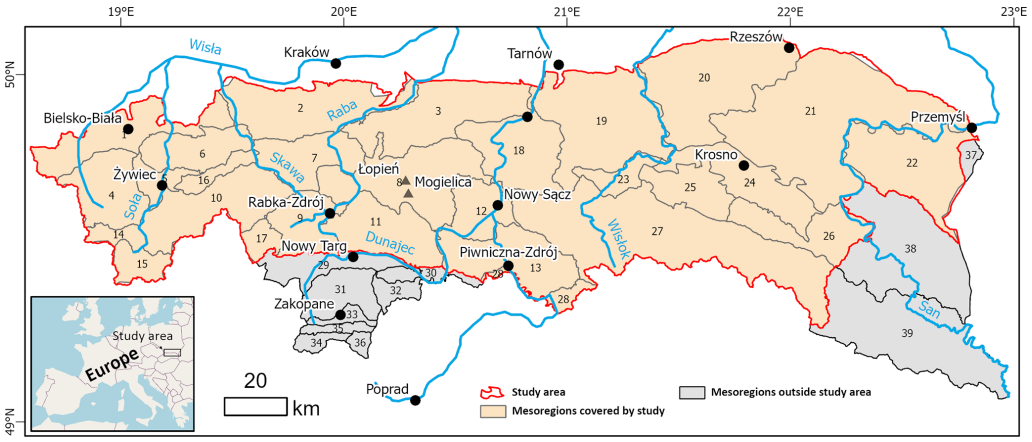

Figure 1. Physio-geographical subdivision of the study area and adjacent parts of the Polish Carpathians based on Solon et al. (2018). Meso-regions covered by the study: 1 – Silesian Foothills; 2 – Wieliczka Foothills; 3 – Wiśnicz Foothills; 4 – Silesian Beskid Mts; 5 – Żywiec Basin; 6 – Mały Beskid Mts; 7 – Makowski Beskid; 8 – Wyspowy Beskid; 9 – Orawa–Jordanów Foothills; 10 – Żywiec–Orawa Beskid Mts; 11 – Gorce Mts; 12 – Sącz Basin; 13 – Sącz Beskid Mts; 14 – Koniaków Intermontane Region; 15 – Żywiec–Kysuce Beskid Mts; 16 – Pewel–Krzeczów ranges; 17 – Orawa Interfluve; 18 – Rożnów Foothills; 19 – Ciężkowice Foothills; 20 – Strzyżów Foothills; 21 – Dynów Foothills; 22 – Przemyśl Foothills; 23 – Gorlice Basin; 24 – Jasło–Krosno Basin; 25 – Jasło Foothills; 26 – Bukowiec Foothills; 27 – Low Beskid Mts; 28 – Poprad Foothills; meso-regions outside the study area: 29 – Orawa–Nowy Targ Basin; 30 – Pieniny Mts; 31 – Fore-Tatra Foothills; 32 – Magura Spiska Mts; 33 – sub-Tatra Depression; 34 – Western Tatra Mts; 35 – Reglowe Tatra Mts; 36 – High Tatra Mts; 37 – Hermanowice Submontane Region; 38 – Sanocko–Turczańskie Mts; 39 – Bieszczady Mts.

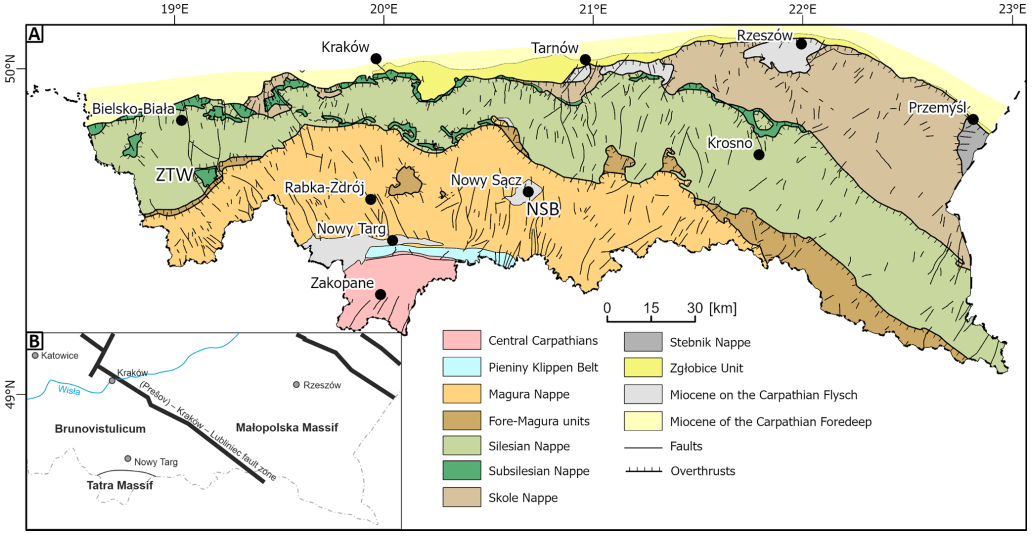

Figure 2. **(a)** Generalized geological map of the Polish part of the Carpathians based on Cieszkowski et al. (2017); faults after Lexa et al. (2000). **(b)** Main tectonic units under the Carpathians, after Żelaźniewicz et al. (2011).

caught. The newly proposed morphostructural subdivision of the Western Carpathians (Minár et al., 2011) is another approach that compiles geological and morphological features. The Polish part of the Western Carpathians is subdivided into the following subregions (numbers according to Minár et al., 2011): (3f) Moravian–Silesian Beskid Mts, (3a) Beskid Żywiecki–Gorce Mts, (3b) Beskid Sądecki–Levočské vrchy Mts, (5a) Beskid Wyspowy Mts, (5b) Low Beskid Mts, and (6) North Foreland. The last subregion spans the entire length of the northern Carpathian boundary between the Orawa and San rivers. We decided to combine the geological subdivision with the morphological one (Solon et al., 2018), which also comprises a subdivision of the outermost units into five sectors (Fig. 3, Table 1). The only change was to include Mount Ciecień in Beskid Wyspowy Mts in the Central Silesian sectors, as this massif, unlike all other peaks in the Beskid Wyspowy Mts, is built of Silesian series deposits (Burtan, 1974).

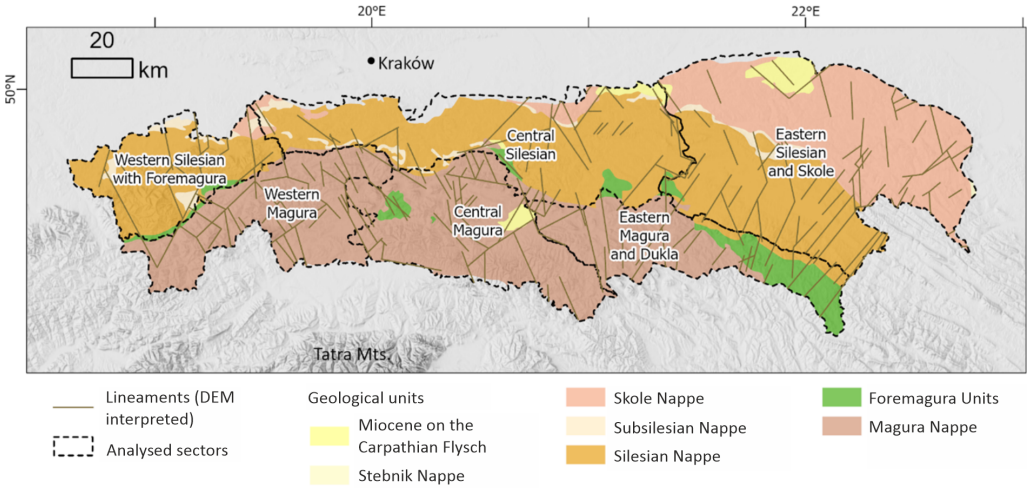

Figure 3. Sectors defined based on the physio-geographical (Solon et al., 2018) and tectonic subdivisions (Golonka et al., 2021) of the study area (Western Outer Carpathians in Poland).

Table 1. Analysed sectors.

Analysed sectors	Symbol	Meso-regions covered according to Solon et al. (2018)
Western Silesian with Fore-Magura	WS	Silesian Beskid Mts, Żywiec Basin, Silesian Foothills, Mały Beskid Mts
Central Silesian	CS	Wieliczka Foothills, Wiśnicz Foothills, Beskid Wyspowy Mts (only the Ciecień Ridge), Rożnów Foothills, Ciężkowice Foothills, Gorlice Basin)
Eastern Silesian and Skole	ES	Przemyśl Foothills, Jasło–Krosno Basin, Strzyżów Foothills, Dynów Foothills, Jasło Foothills, Bukowiec Foothills
Western Magura	WM	Orawa-Jordanów Foothills, Orawa Interfluve, Koniaków Intermontane Region, Żywiec–Kysuce Beskid Mts, Pewel–Krzeczów ranges, Makowski Beskid, Żywiec–Orawa Beskid Mts
Central Magura	CM	Sącz Beskid Mts, Sącz Basin, Wyspowy Beskid (without Ciecień Ridge), Gorce Mts
Eastern Magura and Dukla	EM	Low Beskid Mts

4 Digital elevation model

The Global Multi-resolution Terrain Elevation Data 2010 (GMTED2010, USGS EROS Center, 2023; see Danielson and Gesch, 2011) 7.5 arcsec product was chosen as a working basis. The model is a compilation of different raster-based elevation sources, based mainly on SRTM digital terrain elevation data. The resolution is ca. 0.0021° per pixel, which means ca. 233 m per pixel. This was found to be sufficient, while the working scale during lineament detection was 1 : 150 000. As the shading azimuth can influence the results, the working imagery was multidirectional hillshade (Nagi, 2022).

5 Methods

5.1 Multiple cover lineament detection

The manual method of lineament extraction was applied for two reasons. First, it is the simplest, low cost, and widely used method. The second reason is that it creates a basis for further work, based on automated extraction. However, the method used is prone to some operator-related bias (Scheiber et al., 2015; Ehlen, 2004). Thus, to reduce this bias the lineaments were extracted by two operators working independently, in three sessions, separated by intervals of several months. After each session, the results were analysed and a network of common features was created. Lineaments marked by both operators were merged into single feature. Lineaments marked by only one operator were removed. The

last stage was creating a concise network of lineaments based on the results of the three sessions.

5.2 Network analysis

A network can be described by scale-independent topological characteristics, based on the case of a line network on graph theory. The network (graph) is formed by nodes (end or intersection points) connected by lines (Sanderson and Nixon, 2015; Mukherjee, 2019). The line can be formed by one or more branches connected by nodes. The node can be isolated (I type), an embranchment (Y type), or an intersection (X type), where the latter two types are connecting nodes. Thus, the branch can connect two I-type nodes (I–I branch), isolated and connecting nodes (I–C branch, which can be I–Y or I–X), and two connecting nodes (C–C branch, which can be X–X, X–Y, or Y–Y). The proportion of nodes and branch types can be analysed as tertiary systems that characterize the properties of the network, especially its interconnectivity (Procter and Sanderson, 2018; Sanderson and Nixon, 2015; Sanderson et al., 2018).

The spatial variation in the topological parameters of the network was analysed with the following aspects: (1) regular, in a 5×5 km grid, and (2) within sectors based on the meso-regions of physio-geographical subdivisions, according to Solon et al. (2018), and the main tectonic units (Fig. 3, Table 1).

The NetworkGT QGIS toolbox (Nyberg et al., 2018) was used as a tool in the topological analyses. The lineament network was checked and repaired with NetworkGT tools. An additional stage was the manual correction of some features to eliminate all non-defined types of nodes as well as some extremely short (ca. 500 m or shorter) features. The topological parameters were analysed in three modes: the whole network; the sectors defined; and in a regular 5×5 km grid with a 10 km search radius.

The Rayleigh test of semicircular distribution was performed with the EZ-ROSE spreadsheet (Baas, 2000), and circular statistics were calculated with the SciPy stats module (The SciPy Community, 2022).

6 Results

6.1 Network geometry

The azimuths of the lineaments in all the analysed sectors show a multimodal distribution. Thus, the directions were separated into sets, in a way that gives low values of circular variance. The angular ranges of all the sets are presented in Table 2. For all sets, except for set 2 in the Eastern Magura (EM) sector and set 2 in the Western Silesian (WS) sector, the distribution is not uniform, as checked with the Rayleigh test (Baas, 2000). The two sets not checked were not numerous enough to be representative.

Figure 4. Rose diagrams of the analysed networks in the analytic sectors. Upper row: Western Silesian sector with Fore-Magura (WS), Central Silesia (CS), and Eastern Silesia with Skole (ES); lower row: Western Magura (WM), Central Magura (CM), and Eastern Magura with Dukla (EM). Arrows mark the mean azimuth for the sets defined in Table 2.

The orientation of lineaments in all sectors as well as the circular mean azimuth are shown in Fig. 4. In the Central and Eastern Silesian (CS, ES) and Central and Western Magura sectors (CM, WM), the set 1 mean is located between 34 and 47°, marking a dominant SW–NE strike of lineaments. In the Western Silesian sector (WS), set 1 is oriented more to the north (14°). In all sectors above, there is a second set with a NW–SE trend, mostly oriented at 150–160°, but in the Western Silesian sector case the mean azimuth is lower (127°), as in the case of the first set. The last sector, Eastern Magura and Dukla, is different. There is one dominant set with an azimuth of 62°, and the second set is poorly represented and oriented northward. The angle between the two sets varies in the 62–76° range, except in the Eastern Magura and Dukla sector, where it is only 48°.

6.2 Network topology

In the study area, 305 lineaments were marked in total. These features comprise 432 nodes. Of this count, 58 % are I nodes, 19 % are E nodes, 18 % are Y nodes, and 5 % are X nodes. The network contains 338 branches, of which 49 % are C–I-type branches, 29 % are C–C branches, and 22 % are I–I

Table 2. Azimuths of the lineaments in the analysed sectors. All angles in degrees.

Analysed sector	Set	Azimuth range	*n*	Circular statistics			The acute angle between set means (°)
				Mean	SD	Variance	
CS	1	0–100	15	46.5	14.2	3.5	75.5
	2	100–180	13	151	16.6	4.8	
CM	1	0–80	17	34.1	13	3	63.9
	2	80–180	51	150.2	21.5	8.1	
EM	1	45–75	41	62.1	7.5	1.0	47.7
	2	0–45 75–180	3	14.4	26.7	12.5	
ES	1	0–100	59	42.7	19.7	6.8	62.1
	2	100–180	28	160.6	14.7	3.8	
WM	1	0–100	20	46.5	14.2	3.5	75.5
	2	100–180	40	151	16.6	4.8	
WS	1	0–60 150–180	23	13.6	23.3	9.5	66.2
	2	60–150	5	127.4	8.9	1.4	

branches marking completely separated lineaments. Topological parameters are shown in Table 3.

The highest dimensionless intensity parameter is in the Eastern Magura and Dukla sector (2.05) and the lowest in the Central Silesian sector (0.87). On the other hand, the Eastern Magura sector is characterized by the lowest connections per branch (0.56) or the average degree of the network (1.25) due to its form of mainly parallel features, with only 12 % of the branches of the connecting type (C–C). The best interconnectivity is observed in the Western Silesian sector with 1.62 connections per branch and an average degree of the network of 2.21. This is an effect of the presence of the Żywiec Basin block system in the central part of the region.

The difference between these two (Eastern Magura and Western Silesia) sectors is clearly visible on the ternary diagrams (Fig. 5) presenting the relationships of the nodes and branch types. In the Western Silesian sector, there is a high ratio of Y-type nodes (52 % of non-E-type nodes) and only one I–I branch.

The parameters of all the other sectors fall between the Eastern Magura and Western Silesian sectors. The Western Magura sector has quite good interconnectivity with a similar type of Eastern Magura blocky network.

Another approach to analysing topology is to use a regular sampling grid. The results are shown in Fig. 5 as maps of connections per branch number, 2D network intensity, and dimensionless intensity.

It can be seen we have two relatively large regions with a high value of connections per branch parameter. The first one is in the Western Silesian and partially Western Magura sectors, that is, the Żywiec Basin area, but from a geological point of view there is also a narrow zone of Fore-Magura units occurring between the Silesian and Magura nappes. Moreover, the Sub-Silesian unit tectonic window occurs in this area.

The Nowy Sącz Basin (eastern part of the Central Magura sector in the subdivision used here) is the next region with a high number of connections per network branch. The lineament system in this area surrounds a zone of Neogene deposits lying on the Carpathian flysch and filling the intramountain Nowy Sącz Basin.

The 2D intensity map shows that the Nowy Sącz Basin is characterized in general by a higher intensity than the Żywiec Basin. There is also a general trend towards higher intensity in the western part of the Carpathians (especially the Western Magura and Central Magura sectors) than in the eastern part (Eastern Magura and Dukla).

In terms of dimensionless intensity parameter there are two regions with significantly high values: the south-eastern part of the Wiśnicz Foothills, which are in the Central Silesian sector, and the eastern parts of the Beskid Niski Mts and Bukowiec Foothills in the Eastern Magura and Eastern Silesian sectors, on the geographical border between the Western and Eastern Carpathians.

7 Discussion

7.1 Different lineament identification approaches

There are 110 photo-lineaments marked on the photogeological map of Poland in the studied area (Bażyński et al., 1986). In the same area of the geological map of the Carpathi-

Table 3. Topological parameters of the network in analysed sectors.

	Western Silesia with Fore-Magura	Central Silesia	Eastern Silesia and Skole	Western Magura	Central Magura	Eastern Magura and Dukla	Whole area
	WS	CS	ES	WM	CM	EM	
No. of nodes (I+X+Y)	19	68	101	47	67	40	383
I nodes	8	51	76	26	48	36	293
X nodes	1	6	6	3	6	2	19
Y nodes	10	11	21	18	15	2	71
E nodes	22	38	49	46	61	52	–
C–C connections	11.5	14.5	18.5	21.0	33.5	3.0	77.0
C–I connections	8.5	28.5	35.5	22.0	25.0	11.5	131.0
I–I connections	1.0	11.0	23.5	3.0	14.0	10.5	81.0
No. of branches	21.0	54.0	77.5	46.0	54.5	25.0	291
No. of lines	9.0	31.0	48.5	22.0	31.5	19.0	182
No. of connections	11	17	25	21	19	4	90
Connections per line	2.44	1.10	1.03	1.91	1.21	0.42	0.99
Connections per branch	1.62	1.06	1.02	1.43	1.12	0.56	0.99
Dimensionless intensity	1.21	0.87	1.21	1.65	1.33	2.06	0.75
Avg degree of network	2.21	1.59	1.53	1.96	1.63	1.25	1.52

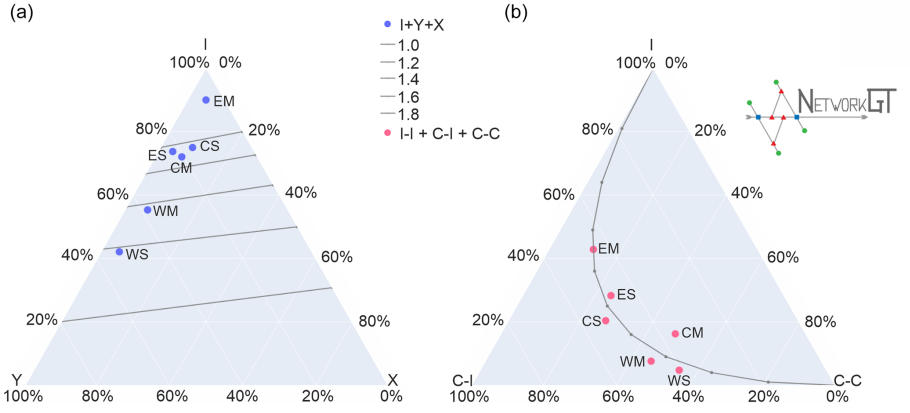

Figure 5. Ternary diagram presenting node **(a)** and branch **(b)** proportions in the analysed sectors.

ans, Lexa et al. (2000) marked 2325 features described as a fault or assumed fault. In many cases, our lineament system seems to be concordant or complementary to that of Lexa et al. (2000) (Fig. 6). In some cases, the features marked as faults are instead thrust lines, as in the Fig. 6a example. The photo-lineament system is in general concordant with the DEM-interpreted system. Visual inspection of the compiled lineament map (Fig. 7a) shows that the NE-striking lineaments of the Eastern Magura sector, in particular, are consistent with each other. Moreover, the system framing the Żywiec tectonic window is visible well in both sets. On the other hand, there are some photo-lineaments that are not recognizable in the DEM and, in fact, also hardly visible on the modern orthophoto map. The most prominent example are two straight, parallel lineaments striking north–north-east in the central part of the study area, cutting across its entire width. These features seem to cut across Gorce Mts; this is not confirmed by our other studies (Kania and Szczęch, 2020; Szczęch and Cieszkowski, 2021). Further to the north, these two lineaments delimit massifs of the Beskid Wyspowy Mts (Mogielica, Łopień). These massifs are in fact particularly visible on the aerial photo, as rather isometric "islands", and are formed by core parts of the synclines (Wójcik et al., 2009). On the other hand, some lineament systems visible well in the DEM are not marked on the photo-lineament map, as in the case of the system north of Nowy Sącz. This shows how these two methods can in fact be recognized as complementary approaches to the lineaments' identification.

The system from the map by Lexa et al. (2000) shows confirmed and inferred faults, which is why it is not fully compatible with lineaments; the lineaments, even when mainly tectonically related, are in fact a broader term (O'Leary et al., 1976). These data, in particular, despite being a very rich collection of features, are not applicable to topological anal-

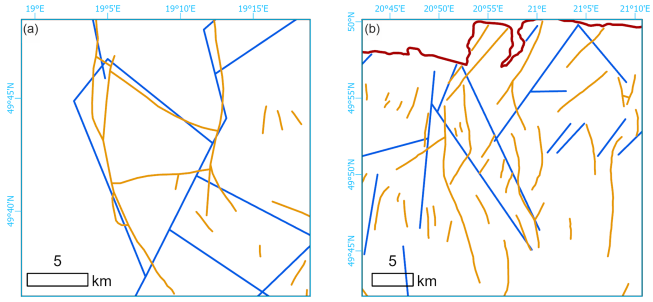

Figure 6. Comparison of the lineament system detected from the GMTED2010 model (blue) and faults by Lexa et al. (2000) (orange). **(a)** Żywiec Basin area. **(b)** Fragment of the Zakliczyn–Olszyny fault zone.

yses: most of the features are short and isolated even when forming a network. Nevertheless, these data include faults that are identified by geological criteria that are not visible in the remote-sensing photo-lineament map (at least at the scale applied in this paper or by Bażyński et al., 1986). These data augment each other, which is highly visible in the Piwniczna-Zdrój area, where DEM interpreted that the NNW-striking lineament along the Poprad River valley (not present in the photo-lineament set) is flanked by a set of N- or NNE-striking faults, which we have not identified in the DEM.

When analysing the distribution of feature azimuth for the whole study area (Fig. 7b–d), it may be noted that the directions for the photo-lineament set (B) and DEM-interpreted set (D) are quite similar. What is noteworthy is the lack of azimuths greater than 150° in the photo set, which are present (albeit in a minority) in the DEM set. Furthermore, the photo set shows two maxima, at ca. 45 and 110°, whilst in the DEM set there are three maxima at ca. 50, 100, and 110°. However, the dominating directions are not in fact distributed uniformly along the W–E span of the Polish Western Carpathians, which can be clearly seen in Fig. 7a, where the domination of NE directions in the eastern sectors may be noticed as well as the presence of two main directions in the western and central sectors.

7.2 Dominating directions of the lineament network

We observed a difference in dominating azimuths of lineaments between the western and central sectors (WS, WM, CS, CM) and eastern sectors (ES, EM) of the study area. The first ones are characterized by two distinct sets of lineaments (NNE or NE and SE), while the second has an SE set that is strongly reduced.

According to the general tectonic model of the Outer Carpathians (Unrug, 1980), the flysch deposits are cut by a set of sinistral strike-slip fault zones. These fault zones are arranged in a fan-like shape along the arc of the Carpathians, leading to the rotation of the set of nappes (Unrug, 1980; Graniczny and Mizerski, 2003). The observed trend towards increasing importance of the NE direction to the east is consistent with this model. However, the more complicated geometry of the western part of the network may be related to the more complicated system of the deep-rooted fault zones in this part (see further discussion below).

7.3 Topological differentiation of the network

There are no topological analyses of the lineament networks for the Outer Carpathians. Our previous article (Kania and Szczęch, 2022) was focused on one mountain massif: Gorce Mts. From the tectonic point of view, this massif is quite homogenous, being located in the one tectono-facial unit (Magura unit) with some subunits within (Bystrica and Krynica subunits). Therefore, the paper focused mainly on different lithostratigraphic units, showing how different types of lithology differ in topology terms.

Scaling the research into the Polish Western Carpathians shows that, in general, there are no differences in the network topology related to the tectono-facial units (Outer Carpathian nappes) since in general, all these units are similar in lithology (flysch packets). However, there are differences related to some irregularities in tectonics: the intra-mountain basins in particular are marked with increased network interconnectivity. The western part of the study area in general has a better-developed network. Especially, the Eastern Magura differs from the rest of the sectors: the domination of one lineament direction results in low network interconnectivity, which is expressed by a high proportion of the I nodes and I–I branches (Fig. 5). We analysed the Magura unit and part of the Dukla unit together; however, the interconnectivity in the Dukla Nappe (belonging to the Fore-Magura group) is stronger than in Magura, which can be related to the proximity of the Silesian unit overthrust.

The highest interconnectivity was observed in the Western Silesian sector. The area is characterized by a high proportion of Y nodes and thus mainly by the presence of C–I or C–C branches (Fig. 5). In the geological context, it is related to the location of the Żywiec tectonic window, which exposes the Sub-Silesian unit. However, the topological study shows that the tectonized zone is wider; the increase in connections per branch zone continues to the south along the Soła River and further, at least to the state border in the Beskid Żywiecki Mts.

7.4 Main large-scale, deep-rooted lineament systems of the Western Carpathians and their relation to DEM-interpreted lineaments

The following, well-known, large-scale lineaments reach the Carpathian basement cutting the Polish part of the Western Outer Carpathians (Doktór et al., 1985): Central Slovakia, Myjava, Muráň, Štítnik, and Przemyśl. There are also lineaments not named by Doktór et al. (1985), but striking paral-

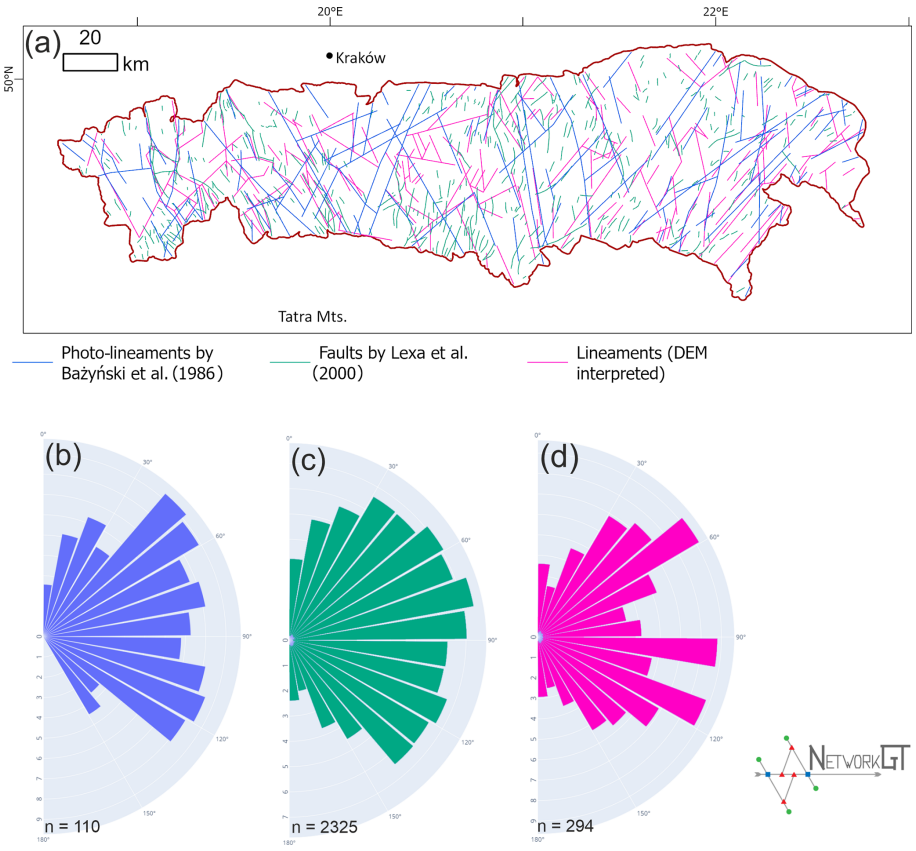

Figure 7. Geometry of lineament networks in the Carpathians. **(a)** Compilation map of lineaments by Bażyński et al. (1986), faults by Lexa et al. (2000), and lineaments interpreted from DEM in the present paper. **(b–d)** Rose diagrams of feature azimuths in the whole study area **(b)** from Bażyński et al. (1986), **(c)** from Lexa et al. (2000), and **(d)** DEM interpreted.

lel, approximately 10 km to the east of the Skawa fault zone (Cieszkowski et al., 2006). Figure 8 presents the generalized positions of the lineaments.

The central Slovak line marks the eastern border of the Żywiec Basin and marks the major fault zone visible well in the displacing Fore–Magura belt near Żywiec. Some of the lineaments belonging to the system can also be traced to the east, with some connecting NE–SW branches near the northern margin of the Carpathians.

The system of Muráň lineaments in the discussed region is marked by a few short NE–SW lineaments in the eastern sectors of the Magura and Silesian units. The Myjava system, in fact one of the most prominent systems in the Carpathians, can be traced along the Nowy Sącz Basin in the study area, continuing to the north where there is a series of short lines parallel to the zone lineaments. The network interconnectivity increases in this area. The lineaments there lie in an extension of the Carpathian Shear Corridor, a large-scale strike-slip zone between Vienna and the High Tatra Mts (Marko et al., 2017). Although the Štítnik system is unclear, some parallel or subparallel lineaments can be assigned to this zone. The Przemyśl lineament zone is identified as a set of long lineaments in the easternmost parts of the area, where the main features of a NE–SW direction are possibly interconnected by shorter N–S lines, forming an interconnected, blocky, two-set system.

Another important deep-rooted linear structure, confirmed by a negative gravimetric anomaly is the Peri-Carpathian line, which runs along the Nowy Sącz–Nowy Targ–Kysucké Nové Mesto line (Zuchiewicz, 1984; Sikora, 1976), which runs similarly to the Myjava structure. The Kraków–Prešov lineament is an extension of the Kraków–Lubliniec fault zone and marks the border between the Małopolska and Brunovistulicum blocks of the basement (Żaba, 1999; Zuchiewicz, 1984). A system of lineaments is clearly visible along this line, mainly in the Magura Nappe; however, parallel photo-lineaments were marked as even longer to the north (Bażyński et al., 1986).

These systems can be arranged into two sets: NNW-, NW–SSE-, SE-striking (Central Slovakia, Skawa, Kraków–Prešov, and Štítnik); and NE–SE (Myjava and Peri-Carpathian, Muráň, and Przemyśl). This implies some points of system intersection, and in the area analysed such a place is in the Nowy Sącz region. This place is characterized by higher interconnection factors (Fig. 9) in relation to the surrounding area. Moreover, in terms of geomorphology, this is

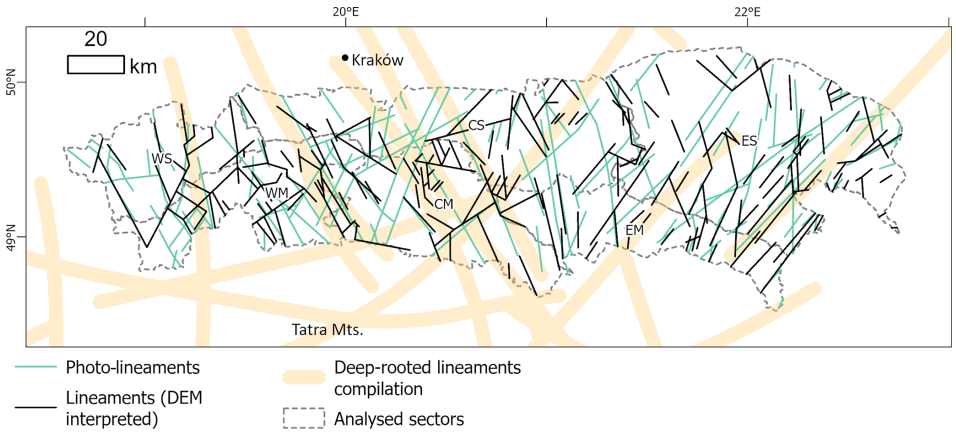

Figure 8. Interpreted lineament system with photo-lineaments by Bażyński et al. (1986) as well as a deep-rooted lineament compilation after Sikora (1976), Zuchiewicz (1984), and Doktór et al. (1985). Important deep-rooted lineaments marked by numbers: 1 – Central Slovakia; 2 – Peri-Carpathian; 3 – Kraków–Prešov; 4 – Štítnik; 5 – Myjava; 6 – Muráň; 7 – Przemyśl.

an intra-mountainous basin, being the only location where deposits are observed in the Magura Nappe Neogene.

The Central Slovakian system strikes along the east border of the Żywiec Basin and Żywiec tectonic window, where the Sub-Silesian Nappe is exposed. We also marked a major lineament there, which is not present on the photo-lineament map (Bażyński et al., 1986) or in the database of the Western Carpathian geological map (Lexa et al., 2000). The lineament (in the central part, the Soła River valley) cuts the Magura Nappe, the Fore-Magura zone with Magura overthrust, and the Silesian Nappe. This structure is one of the edges of the rhomboidal block, in which the Żywiec Basin has been developed. The generally increased degree of network interconnection (Fig. 10) and the intensity of the network in this area can be an effect of the interaction between the Central Slovakian system with the Soła lineament and all the lowered block edges.

The cross-cutting relations of the Myjava lineament and the Štítnik lineament, whose continuation may be the Dunajec fault system, are reflected in the bimodality of lineaments. The dominating maximum in the central Magura sector, at approximately 120°, is similar to the Štítnik lineament; however, the Myjava lineament is reflected there by just a few dominating lineaments, which are relatively long. Moreover, the Peri-Carpathian lineaments are also known in this region. This structure, reflected in the sedimentary cover as the Dunajec fault zone, is also confirmed by a negative gravimetric anomaly (Zuchiewicz, 1984; Sikora, 1976). Another deep structure cutting this area is the Kraków–Prešov fault, which is an extension of the Kraków–Lubliniec fault zone under the Carpathians active to the Quaternary (Żaba, 1999). All these deep cross-cutting features result in an increased degree of the network connectivity observed on the surface. Then, the blocky structure allow the formation of an intramountain basin, filled with Neogene sediments.

Topological analysis also suggests that the well-known Skawa fault zone (Zuchiewicz et al., 2009; Unrug, 1980) is in fact the westernmost part of the wider zone of increased network interconnectivity, extending ca. 10–20 km to the west of the Raba River. The final interpretation of the correlation of lineament-increased interconnectivity areas with tectonic structures of the area is shown in Fig. 10.

The other aspect of the fault system of the Carpathians is occurrence and migration of the mineral waters. The area to the south of Nowy Sącz is a well-known region of CO_2-rich mineral waters with renowned spa sites. These waters are associated with fault zones, often deep ones, penetrating to the crystalline basement of the Carpathians (Oszczypko and Zuber, 2002; Zuber and Chowaniec, 2009; Ciężkowski et al., 2010). It is noteworthy that this region is located on the crossing of two major deep-rooted fault zones: the Štítnik lineament and the Myjava lineament (Fig. 8). Similarly, the deep faults can be an area of migration of hydrocarbons, especially if source rocks are related to the platform cover of the Brunovistulicum and the Małopolska Massif lying under the Carpathians. In fact, some of the Polish Carpathian gas deposits are related to the Mesozoic–Palaeozoic basement (Kotarba and Koltun, 2006). Thus, the analysis of the fault systems and their interconnectivity has potential in the study of both hydrocarbon and hydrogeological systems.

8 Conclusions

The proposed data source and analysis method complement other lineament analyses from the study area. The observed azimuths are in general concordant with the photo-lineament network; however, there are some structures that are not confirmed by DEM interpretation. The relationship between the DEM-interpreted data and geologically confirmed faults

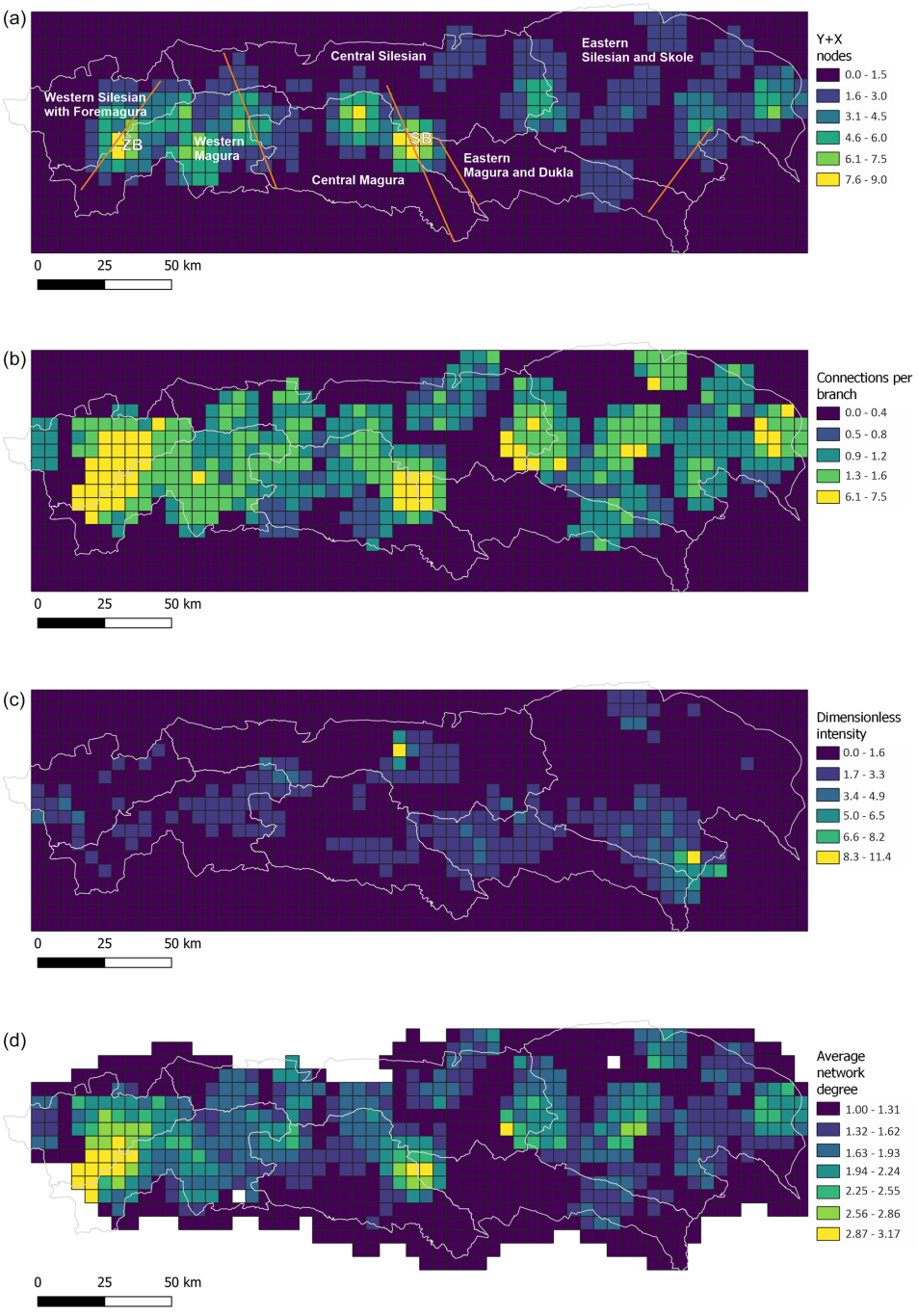

Figure 9. Topological parameters of the lineament network, from top to bottom: connecting node number, connections per branch number, dimensionless intensity factor, and average network degree. ZB – Żywiec Basin (Żywiec tectonic window); SB – Nowy Sącz Basin; lines on X–Y nodes map are main faults.

shows the usefulness of DEM as a data source in fault detection.

The dominating directions of the network are typical of the Western Carpathians, with a clear increase in the proportion of NE-striking features towards the east.

The topological properties of the lineament network in the Western Carpathians show E–W trends but no clear S–N (perpendicular to the tectonic units) trends. This justifies the proposed subdivision of the Carpathians into the western, central and eastern sectors in addition to the tectonofacial subdivision. The eastern sectors are dominated by NE–

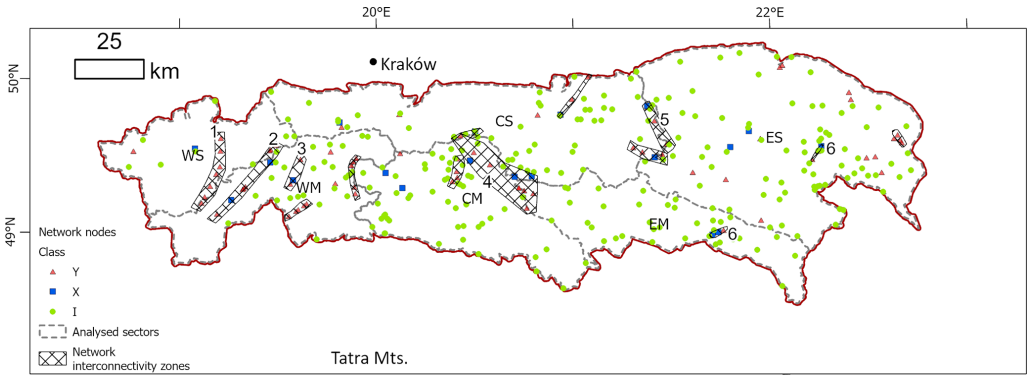

Figure 10. Network nodes and zones of interconnectivity and their interpretation in the context of Outer Carpathians nappes (surface) and basement (deep) tectonics. 1 – Soła fault zone (surface); Central Slovakia lineament (deep); 2 – fault system along Sopotnia Valley; 3 – Skawa fault zone (surface); 4 – Nowy Sącz Basin (surface), Kraków–Prešov, Myjava and Štítnik lineaments (deep); 5 – faults along Wisłoka Valley (surface); 6 – Muráň lineament (deep).

SW trends and low interconnectivity, while the central and western sectors are more interconnected and characterized by cross-cutting relationships of the two main lineament directions. The degree of network interconnectivity increases in areas with a lower morphology (intra-mountainous basins): the Żywiec Basin and the Nowy Sącz Basin.

The geometry of the network, in general, reflects a system of deep-rooted lineaments. The cross-cutting area of the main deep lineaments is reflected in stronger network interconnectivity in the Nowy Sącz area.

Code availability. The NetworkGT toolbox is available at https://github.com/BjornNyberg/NetworkGT (DOI: https://doi.org/10.1130/GES01595.1, Nyberg et al., 2018). SciPy is available at https://github.com/scipy/scipy (The SciPy Community, 2022; Virtanen et al., 2020).

Data availability. The GMTED2010 digital elevation model is available at https://doi.org/10.5066/F7J38R2N (USGS EROS Center, 2023).

Author contributions. MK: conceptualization, methodology, formal analysis, investigation, writing (original draft), visualization. MS: investigation, writing (review and editing), visualization.

Competing interests. The contact author has declared that neither of the authors has any competing interests.

Acknowledgements. The authors would like to thank both referees, Fabrizio Balsamo and Jan Golonka, for their helpful comments that improved a quality of the paper.

Financial support. The publication and proofreading of this publication has been supported by a grant from the Priority Research Area (Digiworld) under the Strategic Programme Excellence Initiative at Jagiellonian University.

Review statement. This paper was edited by Arjen Stroeven and reviewed by Jan Golonka and Fabrizio Balsamo.

References

Baas, J. H.: EZ-ROSE: a computer program for equal-area circular histograms and statistical analysis of two-dimensional vectorial data, Comput. Geosci., 26, 153–166, https://doi.org/10.1016/S0098-3004(99)00072-2, 2000.

Barmuta, J., Starzec, K. and Schnabel, W.: Seismic-Scale Evidence of Thrust-Perpendicular Normal Faulting in the Western Outer Carpathians, Poland, Minerals, 11, 1252, https://doi.org/10.3390/min11111252, 2021.

Bażyński, J., Doktór, S., and Graniczny, M.: Mapa fotogeologiczna Polski w skali 1:1 000 000, Wydawnictwa Geologiczne, Warszawa, 1986.

Burtan, J.: Detailed Geological Map of Poland, 1:50 000 scale, Mszana Dolna sheet (1016), Wydawnictwa Geologiczne, Warszawa, 1974.

Chodyń, R.: Zastosowanie cyfrowego modelu terenu (DEM) w badaniach geologicznych na przykładzie obszaru między Dobczycami a Mszaną Dolną (polskie Karpaty zewnętrzne), Przegląd Geologiczny, 52, 315–320, 2004.

Cieszkowski, M., Golonka, J., Waśkowska-Oliwa, A., and Chrustek, M.: Budowa geologiczna rejonu Sucha Beskidzka – Świnna Poręba (polskie Karpaty fliszowe), Geologia/Akademia Górniczo-Hutnicza im. Stanisława Staszica w Krakowie, 32, 155–201, 2006.

Cieszkowski, M., Kysiak, T., Szczęch, M., and Wolska, A.: Geology of the Magura Nappe in the Osielec area with emphasis on an Eocene olistostrome with metabasite olistoliths

(Outer Carpathians, Poland), Ann. Soc. Geol. Pol., 87, 169–182, https://doi.org/10.14241/asgp.2017.009, 2017.

Ciężkowski, W., Chowaniec, J., Górecki, W., Krawiec, A., Rajchel, L. and Zuber, A.: Mineral and thermal waters of Poland, Przegląd Geologiczny, 58, 762–773, 2010.

Danielson, J. J. and Gesch D. B.: Global Multi-resolution Terrain Elevation Data 2010 (GMTED2010), Open-File Report 2011–1073, U.S. Geological Survey, 26 pp., 2011.

Doktór, S. and Graniczny, M.: Geologiczna interpretacja zdjęć satelitarnych i radarowych wschodniej części Karpat, Kwartalnik Geologiczny, 26, 231–245, 1982.

Doktór, S. and Graniczny, M.: Fotogeologiczna analiza zdjęć satelitarnych Karpat, Kwartalnik Geologiczny, 27, 645–656, 1983.

Doktór, S., Dornič, J., Graniczny, M., and Reichwalder, P.: Structural elements of Western Carpathians and their Foredeep on the basis of satellite interpretation, Geol. Q., 29, 129–138, 1985.

Doktór, S., Graniczny, M., Kucharski, R., Molek, M., and Dąbrowska, B.: Wgłębna budowa geologiczna Karpat w świetle kompleksowej analizy teledetekcyjno-geofizycznej, Przegląd Geologiczny, 38, 469–475, 1990.

Doktór, S., Graniczny, M., Kowalski, Z., and Wójcik, A.: Możliwości zastosowania wyników interpretacji zdjęć radarowych do analizy tektonicznej Karpat, Przegląd Geologiczny, 50, 852–860, 2002.

Ehlen, J.: Lineation, edited by: Goudie, A. S., Encyclopedia of Geomorphology, Routledge Ltd, New York, 2, 623–624, ISBN 0-415-27298-X, 2004.

Golonka, J., Aleksandrowski Paweł, Aubrecht, R., Chowaniec, J., Chrustek, M., Cieszkowski, M., Florek, R., Gawęda, A., Jarosiński, M., Kępińska, B., and others: The Orava deep drilling project and post-Palaeogene tectonics of the northern Carpathians, Ann. Soc. Geol. Pol., 75, 211–248, 2005.

Golonka, J., Waśkowska, A., and Ślączka, A.: The Western Outer Carpathians: Origin and evolution, Z. Dtsch Ges. Geowiss., 170, 229–254, 2019.

Golonka, J., Gawęda, A., and Waśkowska, A.: Carpathians, Reference Module in Earth Systems and Environmental Sciences, in: Encyclopedia of Geology, edited by: Alderton, D. and Elias, S. A., 2nd Edn., Academic Press, 372–381, https://doi.org/10.1016/b978-0-12-409548-9.12384-x, 2021.

Graniczny, M. and Mizerski, W.: Lineamenty na zdjęciach satelitarnych Polski – próba podsumowania, Przegląd Geologiczny, 51, 474–482, 2003.

Kania, M. and Szczęch, M.: Geometry and topology of tectonolineaments in the Gorce Mts. (Outer Carpathians) in Poland, J. Struct. Geol., 141, 104186, https://doi.org/10.1016/j.jsg.2020.104186, 2020.

Kania, M. and Szczęch, M.: Tectonic Structures Interpretation Using Airborne-Based LiDAR DEM on the Examples from the Polish Outer Carpathians, in: Atlas of Structural Geological and Geomorphological Interpretation of Remote Sensing Images, edited by: Misra, A. A. and Mukherjee, S., John Wiley & Sons, 157–165, ISBN 1119813352, 2022.

Kotarba, M. J. and Koltun, Y. V.: The Origin and habitat of hydrocarbons of the Polish and Ukrainian parts of the Carpathian Province, in: Golonka, J. and Picha, F., The Carpathians and Their Foreland: Geology and Hydrocarbon Resources: AAPG Memoir, 84, 321–368, 2006.

Książkiewicz, M.: The Tectonics of the Carpathians, in: Geology of Poland, vol. 4. Tectonics, The Alpine Tectonic Epoch, Geological Institute, Warszawa, 476–608, 1977.

Leech, D. P., Treloar, P. J., Lucas, N. S., and Grocott, J.: Landsat TM analysis of fracture patterns: A case study from the Coastal Cordillera of northern Chile, Int. J. Remote Sens., 24, 3709–3726, https://doi.org/10.1080/0143116031000102520, 2003.

Lexa, J., Bezaìk, V., Elečko, M., Mello, J., Polaìk, M., and Vozaìr, J.: Geological map of western Carpathians and adjacent areas 1:500 000, S˘ta´tny geologicky´ u´stav Diony´za S˘tu´ra, Bratislava, 2000.

Mahel', M.: Tectonics of the Carpathian–Balkan Regions, Explanations to the Tectonic Map of the Carpathian-Balkan Regions and Their Foreland, Štátny geologický ústav Dionýza Štúra, Bratislava, 180–197, 1974.

Marko, F., Andriessen, P. A. M., Tomek, Č., Bezák, V., Fojtíková, L., Bošanský, M., Piovarči, M., and Reichwalder, P.: Carpathian Shear Corridor – A strike-slip boundary of an extruded crustal segment, Tectonophysics, 703–704, 119–134, https://doi.org/10.1016/j.tecto.2017.02.010, 2017.

Minár, J., Bielik, M., Kováč, M., Plašienka, D., Barka, I., Stankoviansky, M., and Zeyen, H.: New morphostructural subdivision of the Western Carpathians: An approach integrating geodynamics into targeted morphometric analysis, Tectonophysics, 502, 158–174, 2011.

Motyl-Rakowska, J. and Ślączka, A.: Ważniejsze lineamenty Karpat i ich związek ze znanymi uskokami, Przegląd Geologiczny, 32, 72–77, 1984.

Mukherjee, S.: Using Graph Theory to Represent Brittle Plane Networks, in: Developments in Structural Geology and Tectonics, Elsevier, Vol. 5, 259–271, https://doi.org/10.1016/B978-0-12-814048-2.00022-3, 2019.

Nagi, R.: Introducing Esri's Next Generation Hillshade, https://www.esri.com/arcgis-blog/products/arcgis-living-atlas/imagery/introducing-esris-next-generation-hillshade/?rmedium=redirect&rsource=blogs.esri.com/esri/arcgis/2014/07/14/introducing-esris-next-generation-hillshade, last access: 1 June 2022.

Nyberg, B., Nixon, C. W., and Sanderson, D. J.: NetworkGT: A GIS tool for geometric and topological analysis of two-dimensional fracture networks, Geosphere [code], 14, 1618–1634, https://doi.org/10.1130/GES01595.1, 2018.

O'Leary, D. W., Friedman, J. D., and Pohn, H. A.: Lineament, linear, lineation: Some proposed new standards for old terms, Geol. Soc. Am. Bull., 87, 1463–1469, 1976.

Oszczypko, N.: Late Jurassic-Miocene evolution of the Outer Carpathian fold-and-thrust belt and its foredeep basin (Western Carpathians, Poland), Geol. Q., 50, 169–194, 2006.

Oszczypko, N. and Zuber, A.: Geological and isotopic evidence of diagenetic waters in the Polish Flysch Carpathians, Geol. Carpath., 53, 257–268, 2002.

Ozimkowski, W.: Lineamenty otoczenia Tatr – porównanie interpretacji DEM i MSS, Przegląd Geologiczny, 56, 1099–1102, 2008.

Plašienka, D.: Continuity and episodicity in the early Alpine tectonic evolution of the Western Carpathians: How large-scale processes are expressed by the orogenic architecture and rock record data, Tectonics, 37, 2029–2079, 2018.

Procter, A. and Sanderson, D. J.: Spatial and layer-controlled variability in fracture networks, J. Struct. Geol., 108, 52–65, https://doi.org/10.1016/j.jsg.2017.07.008, 2018.

Sanderson, D. J. and Nixon, C. W.: The use of topology in fracture network characterization, J. Struct. Geol., 72, 55–66, https://doi.org/10.1016/j.jsg.2015.01.005, 2015.

Sanderson, D. J., Peacock, D. C. P., Nixon, C. W., and Rotevatn, A.: Graph theory and the analysis of fracture networks, J. Struct. Geol., 125, 155–165, https://doi.org/10.1016/j.jsg.2018.04.011, 2018.

Scheiber, T., Fredin, O., Viola, G., Jarna, A., Gasser, D., and Łapińska-Viola, R.: Manual extraction of bedrock lineaments from high-resolution LiDAR data: methodological bias and human perception, GFF, 137, 362–372, https://doi.org/10.1080/11035897.2015.1085434, 2015.

Sikora, R.: Geological and geomorphological conditions of landslide development in the Wisła source area of the Silesian Beskid mountains (Outer Carpathians, southern Poland), Geol. Q., 66, 19, 2022.

Sikora, W.: On lineaments found in the Carpathians, Rocznik Polskiego Towarzystwa Geologicznego, 46, 3–37, 1976.

Ślączka, A., Kruglov, S., Golonka, J., Oszczypko, N., and Popadyuk, I.: Geology and hydrocarbon resources of the Outer Carpathians, Poland, Slovakia, and Ukraine: general geology, in: The Carpathians and Their Foreland: Geology and Hydrocarbon Resources: AAPG Memoir, edited by: Golonka, J. and Picha, F., 84, 221–258, https://doi.org/10.1306/M84985, 2006.

Solon, J., Borzyszkowski, J., Małgorzata Bidłasik, Richling, A., Badora, K., Balon, J., Brzezińska-Wójcik, T., Chabudziński, Ł., Dobrowolski, R., Grzegorczyk, I., Jodłowski, M., Kistowski, M., Kot, R., Krąż, P., Lechnio, J., Macias, A., Majchrowska, A., Malinowska, E., Migoń, P., Myga-Piątek, U., Nita, J., Papińska, E., Rodzik, J., Strzyż, M., Terpiłowski, S., Ziaja, W., and Paul, J.: Physico-geographical mesoregions of Poland: verification and adjustment of boundaries on the basis of contemporary spatial data, Geographia Polonica, 91, 143–170, https://doi.org/10.7163/GPol.0115, 2018.

Szczęch, M. and Cieszkowski, M.: Geology of the Magura Nappe, south-western Gorce Mountains (Outer Carpathians, Poland), J. Maps, 17, 453–464, https://doi.org/10.1080/17445647.2021.1950579, 2021.

Teisseyre, W.: O związku w budowie tektonicznej Karpat i ich przedmurza, Kosmos, 32, 393–402, 1907.

The SciPy Community: SciPy (scipy.stats) v 1.9.3 Manual: https://docs.scipy.org/doc/scipy/tutorial/stats.html, last access: 8 November 2022.

Thiele, S. T., Jessell, M. W., Lindsay, M., Ogarko, V., Wellmann, J. F., and Pakyuz-Charrier, E.: The topology of geology 1: Topological analysis, J. Struct. Geol., 91, 27–38, https://doi.org/10.1016/J.JSG.2016.08.009, 2016.

Unrug, R.: Tectonic rotation of flysch nappes in the Polish Outer Carpathians, Rocznik Polskiego Towarzystwa Geologicznego, 50, 27–39, 1980.

USGS EROS Center: Digital Elevation – Global Multi-resolution Terrain Elevation Data 2010 (GMTED2010), USGS EROS Center [data set], https://doi.org/10.5066/F7J38R2N, last access: 2 May 2023.

Valentini, L., Perugini, D., and Poli, G.: The "small-world" topology of rock fracture networks, Physica A, 377, 323–328, https://doi.org/10.1016/j.physa.2006.11.025, 2007.

Van der Meer, F. D., van der Werff, H. M. A., van Ruitenbeek, F. J. A., Hecker, C. A., Bakker, W. H., Noomen, M. F., van der Meijde, M., Carranza, E. J. M., de Smeth, J. B., and Woldai, T.: Multi- and hyperspectral geologic remote sensing: A review, Int. J. Appl. Earth Obs. Geoinf., 14, 112–128, https://doi.org/10.1016/j.jag.2011.08.002, 2012.

Virtanen, P., Gommers, R., Oliphant, T. E. et al.: SciPy 1.0: fundamental algorithms for scientific computing in Python, Nat. Methods, 17, 261–272, https://doi.org/10.1038/s41592-019-0686-2, 2020 (code available at: https://github.com/scipy/scipy, last access: 8 May 2023).

Wójcik, A., Czerwiec, J., and Krawczyk, M.: Szczegółowa Mapa Geologiczna Polski 1:50 000, arkusz Limanowa, (1017), Państwowy Instytut Geologiczny, Warszawa, 2009.

Yang, L., Meng, X., and Zhang, X.: SRTM DEM and its application advances, Int. J. Remote Sens., 32, 3875–3896, https://doi.org/10.1080/01431161003786016, 2011.

Zuber, A. and Chowaniec, J.: Diagenetic and other highly mineralized waters in the Polish Carpathians, Appl. Geochem., 24, 1889–1900, 2009.

Zuchiewicz, W.: The late Neogene – Quaternary tectonic mobility of the Polish West Carpathians – a case study of the Dunajec drainage basin, Ann. Soc. Geol. Pol., 54, 133–189, 1984.

Zuchiewicz, W., Tokarski, A. K., Świerczewska, A., and Cuong, N. Q.: Neotectonic Activity of the Skawa River Fault Zone (Outer Carpathians, Poland), Ann. Soc. Geol. Pol., 79, 67–93, 2009.

Żaba, J.: Ewolucja strukturalna utworów dolnopaleozoicznych w strefie granicznej bloków górnośląskiego i małopolskiego, Prace Państwowego Instytutu Geologicznego, 166, 1–162, 1999.

Żelaźniewicz, A., Aleksandrowski, P., Buła, Z., Kornkowski, P. H., Konon, A., Oszczypko, N., Ślączka, A., Żaba, J. and Żytko, K.: Regionalizacja Tektoniczna Polski, Komitet Nauk Geologicznych PAN, Wrocław, 1–60, ISBN 978-83-63377-01-4, 2011.